

1 **A divergent *Articulavirus* in an Australian gecko identified using**
2 **meta-transcriptomics and protein structure comparisons**

3

4

5

6 Ayda Susana Ortiz-Baez¹, John-Sebastian Eden^{1,2}, Craig Moritz³ and Edward C. Holmes^{1*}

7

8

9

10 ¹Marie Bashir Institute for Infectious Diseases and Biosecurity, School of Life and
11 Environmental Sciences and School of Medical Sciences, The University of Sydney,
12 Sydney, New South Wales 2006, Australia.

13 ²Centre for Virus Research, Westmead Institute for Medical Research, Westmead, NSW
14 2145, Australia.

15 ³Research School of Biology & Centre for Biodiversity Analysis, The Australian National
16 University, Acton, ACT 6201, Australia.

17

18

19 *Correspondence: edward.holmes@sydney.edu.au

20

21 **Keywords:** virus discovery; protein structure; meta-transcriptomics; *Tilapia tilapinevirus*;
22 *Articulavirales*; *Amnoonviridae*; RNA virus; gecko

23 **Abstract**

24 The discovery of highly divergent RNA viruses is compromised by their limited sequence
25 similarity to known viruses. Evolutionary information obtained from protein structural
26 modelling offers a powerful approach to detect distantly related viruses based on the
27 conservation of tertiary structures in key proteins such as the viral RNA-dependent RNA
28 polymerase (RdRp). We utilised a template-based approach for protein structure
29 prediction from amino acid sequences to identify distant evolutionary relationships among
30 viruses detected in meta-transcriptomic sequencing data from Australian wildlife. The
31 best predicted protein structural model was compared with the results of similarity
32 searches against protein databases based on amino acid sequence data. Using this
33 combination of meta-transcriptomics and protein structure prediction we identified the
34 RdRp (PB1) gene segment of a divergent negative-sense RNA virus in a native Australian
35 gecko (*Geyra lauta*) that was confirmed by PCR and Sanger sequencing. Phylogenetic
36 analysis identified the *Gecko articulavirus* (GECV) as a newly described genus within the
37 family *Amnoonviridae*, order *Articulavirales*, that is most closely related to the fish virus
38 *Tilapia tilapinevirus* (TiLV). These findings provide important insights into the evolution of
39 negative-sense RNA viruses and structural conservation of the viral replicase among
40 members of the order *Articulavirales*.

41 Introduction

42 The development of next-generation sequencing technologies (NGS), including total RNA
43 sequencing (meta-transcriptomics), has revolutionized studies of virome diversity and
44 evolution [1–3]. Despite this, the discovery of highly divergent viruses remains challenging
45 because of the often limited (or no) primary sequence similarity between putative novel
46 viruses and those for which genome sequences are already available [4–6]. For example,
47 it is possible that the small number of families of RNA viruses found in bacteria, as well as
48 their effective absence in archaeobacteria, in reality reflects the difficulties in detecting
49 highly divergent sequences rather than their true absence from these taxa [3].

50 The conservation of protein structures in evolution and the limited number of proteins
51 folds (fold space) in nature form the basis of template-based protein structure prediction
52 [7], providing a powerful way to reveal the origins and evolutionary history of viruses [8,9].
53 Indeed, the utility of protein structural similarity in revealing key aspects of virus evolution
54 is well known [9,10]. For instance, double-strand (ds) DNA viruses including the
55 thermophilic archaeal virus STIV, enterobacteria phage PRD1, and human adenovirus
56 exhibit conserved viral capsids, suggesting a deep common ancestry [11]. Thus, protein
57 structure prediction utilising comparisons to solved protein structures can assist in the
58 identification of potentially novel viruses [7,12]. Herein, we use this method as an
59 alternative approach to virus discovery.

60 There is a growing availability of three-dimensional structural data in curated
61 databases such as the Protein Data Bank (PDB), with approximately 11,000 viral protein
62 solved structures that can be used in comparative studies. Importantly, these include
63 structures of the RNA-dependent RNA polymerase (RdRp) that exhibits the highest level
64 of sequence similarity among RNA viruses, including a number of key conserved motifs,
65 and hence is expected to contain relatively well conserved protein structures. Exploiting
66 such structural features in combination with metagenomic data will undoubtedly improve
67 our ability to detect divergent viruses in nature, particularly in combination with wildlife
68 surveillance [2,4,13].

69 The International Committee on Taxonomy of Viruses (ICTV) recently introduced the
70 *Amnoonviridae* as a newly recognized family of negative-strand RNA viruses present in
71 fish (ICTV Master Species List 2018b.v2). Together with the *Orthomyxoviridae*, the
72 *Amnoonviridae* are classified in the order *Articulavirales*, describing a set of negative-
73 sense RNA viruses with segmented genomes. While the *Orthomyxoviridae* includes seven
74 genera, four of these comprise influenza viruses (FLUV), and to date the family
75 *Amnoonviridae* comprises a single genus – *Tilapinevirus* – which in turn includes only a
76 single species – *Tilapia tilapinevirus* or Tilapia Lake virus (TiLV).

77 TiLV was originally identified in farmed tilapine populations (*Oreochromis niloticus*) in
78 Israel and Ecuador [14]. The virus has now been described in wild and hybrid tilapia
79 across several countries in the Americas, Africa, Asia, and Southeast Asia [15–17]. TiLV
80 has been associated with high morbidity and mortality in infected animals. Pathological
81 manifestations include syncytial hepatitis, skin erosion and encephalitis [15,18]. TiLV was
82 initially classified as a putative orthomyxo-like virus based on weak sequence
83 resemblance (~17% amino acid identity) in the PB1 segment that contains the RdRp, as
84 well as the presence of conserved 5' and 3' termini [14]. While both the *Orthomyxoviridae*
85 and *Amnoonviridae* have negative-sense, segmented genomes, the genomic organization
86 of the *Amnoonviridae* comprises 10 instead of 7-8 segments [14,18,19], and their
87 genomes are shorter (~10 kb) than those of the *Orthomyxoviridae* (~12-15 kb). To date,
88 however, only the RdRp (encoded by a 1641 bp PB1 sequence) has been reliably defined,
89 and most segments carry proteins of unknown function. Importantly, comparisons of TiLV
90 RdRp with sequences from members of the *Orthomyxoviridae* revealed the presence of
91 four conserved amino acid motifs (I-IV) of size 4-9 amino acid residues each [14] that
92 effectively comprise a "molecular fingerprint" for the order.

93 Unlike other members of the *Articulavirales* [20], TiLV appears to have a limited host
94 range and has been only documented in tilapia (*O. niloticus*, *O. sp.*) and hybrid tilapia (*O.*
95 *niloticus* x *O. aureus*). Herein, we report the discovery of a divergent virus from an
96 Australian gecko (*Geyra lauta*) using a combination of meta-transcriptomic and structure-
97 based approaches, and employ a phylogenetic approach to reveal its relationship to TiLV.
98 Our work suggests that this Gecko virus likely represents a novel genus within the
99 *Amnoonviridae*.

100 **Materials and Methods**

101 *Sample collection*

102 A total of seven individuals corresponding to the reptile species *Carlia amax*, *Carlia*
103 *gracilis*, *Carlia munda*, *Gehyra lauta*, *Gehyra nana*, *Heteronotia binoei*, and *Heteronotia*
104 *planiceps* were collected alive in 2013 from Queensland, Australia. Specimens were
105 identified by mtDNA typing and/or morphological data. Livers were harvested and stored
106 in RNAlater at -80°C before downstream processing. All sampling was conducted in
107 accordance with animal ethics approval (#A2012/14) from the Australian National
108 University and collection permits from the Parks and Wildlife Commission of the Northern
109 Territory (#45090), the Australian Government (#AU-COM2013-192), and the Department
110 of Environment and Conservation (#SF009270).

111 *Sampling processing and sequencing*

112 RNA extraction was performed using the RNeasy Plus minikit (Qiagen) following
113 manufacturer's instructions. Each of the seven livers were extracted individually and then
114 pooled in equal amounts. For RNA sequencing, ribosomal RNA (rRNA) was depleted
115 using the RiboZero (epidemiology) depletion kit and libraries were prepared with the
116 TruSeq stranded RNA library prep kit before sequencing on an Illumina HiSeq 2500
117 platform (100 bp paired end reads). Library preparation and sequencing was performed
118 by the Australian Genome Research Facility (AGRF), generating a total of 22,394,787
119 paired end reads for the pooled liver RNA library.

120 *De novo assembly and sequence annotation*

121 Raw Illumina reads were trimmed of sequencing adapters and low-quality bases with
122 Trimmomatic v0.38 [21]. The trimmed reads were then *de novo* assembled into contigs
123 (transcripts) using Trinity v2.8.6 [22]. Contig abundance was estimated with RSEM [23]
124 and shown as the numbers of transcripts per million (TPM). For sequence annotation,
125 contigs were compared against the NCBI nucleotide (nt) and non-redundant (nr) protein
126 databases (nr) using BLASTn [24] and DIAMOND [25], respectively.

127 *Protein structure prediction for virus detection*

128 To further screen the meta-transcriptomic data, all the assembled sequences below
129 the assigned threshold ($e\text{-value} \geq 10^{-5}$) were assigned as "orphan" contigs ($n=293,586$).
130 These were then analysed using a protein structure-informed approach. Specifically,
131 orphan contigs were translated into all six open reading frames (ORFs) using the getorf
132 program [26] to identify continuous ORFs of at least 1000nt in length between two stop
133 codons ($n=57$). To detect distant sequence homologies and predict viral protein
134 structures, this subset of translated ORFs were then analysed using a template-based
135 modelling approach as implemented in Phyre2 (<http://www.sbg.bio.ic.ac.uk/phyre2>) [27].
136 In brief, target proteins were compared against proteins of known structure via homology
137 modelling and fold recognition, followed by loop modelling and sidechain fitting [27].
138 Confident matches (confidence $>90\%$) to known viral structures were selected for
139 downstream analyses. Annotations from the predicted model were used as preliminary
140 data for tentative taxonomic assignment and protein classification.

141 *Annotation of the newly discovered virus*

142 To further corroborate the viral origin of the predicted protein structure and gain
143 insights into its taxonomic classification, we conducted parallel comparisons using

144 DIAMOND [25] against the GenBank non-redundant (nr) database
145 (<https://www.ncbi.nlm.nih.gov/>) and the HMMER web server
146 (<http://www.ebi.ac.uk/Tools/hmmer>) against the following profile databases: (i) reference
147 proteomes (<https://proteininformationresource.org/rps/>), (ii) Uniprot
148 (<https://www.uniprot.org/>) and (iii) Pfam (<https://pfam.xfam.org/>). In addition, conserved
149 domains were annotated using the Conserved Domain Database (CDD) and the CD-
150 search tool (<http://www.ncbi.nlm.nih.gov/Structure/cdd/cdd.shtml>). To detect additional
151 contigs and better characterize the entire genome of the novel virus, we aligned the DNA
152 contigs against custom databases using DIAMOND [25], including (i) a reference RdRp
153 sequences from the order *Articulavirales*, and (ii) reference sequences corresponding to
154 all the segments of TiLV (Table S1). Given the divergent nature of the viruses, we
155 considered all hits with E-value $>10^{-4}$.

156 *Phylogenetic analysis*

157 The predicted contig encoding the RdRp of the newly discovered virus was aligned
158 with reference protein sequences of the order *Articulavirales* (Table S2). A multiple amino
159 acid sequence alignment was performed using the E-INS-i algorithm as implemented in
160 the MAFFT v7.450 program [28]. Selection of the best-fit model of amino acid substitution
161 was carried out using the Akaike Information criterion (AIC) and the Bayesian Information
162 Criterion (BIC) with the standard model selection option (-m TEST) in IQ-TREE [29].
163 Phylogenetic analysis of these data was then performed using the Maximum Likelihood
164 (ML) method available in IQ-TREE, with node support estimated with the ultra-fast
165 bootstrap (UFBoot) approximation (1000 replicates) and the Shimodaira-Hasegawa
166 approximate Likelihood ratio test (SH-aLRT). Sequencing reads are available at the NCBI
167 Sequence Read Archive (SRA) under the Bioproject PRJNA626677 (BioSample:
168 SAMN14647831; Sample name: VERT7; SRA: SRS6507258). The assembled sequence
169 for GECV was deposited in GenBank under the accession number MT386081.

170 *PCR validation*

171 To validate the presence of the novel gecko amnoonvirus, and to identify the putative
172 host species, we screened the individual liver RNA using RT-PCR. Briefly, cDNA was
173 prepared using Superscript IV VILO master mix and RT-PCR was performed with the
174 Platinum SuperFi Green PCR master mix and two primers sets targeting the gecko RdRp
175 contig – F2V7 and F3V7 (Table S3). The resultant RT-PCR products were analysed by
176 agarose gel electrophoresis and validated by Sanger sequencing.

177 **Results**

178 *Virus discovery using meta-transcriptomics and protein structural features*

179 We used a meta-transcriptomic approach to screen a single pooled library containing
180 liver RNA of seven Australian native reptile species (*Gehyra lauta*, *Carlia amax*,
181 *Heteronotia binoei*, *Gehyra nana*, *Carlia gracilis*, *Carlia munda*, and *Heteronotia planiceps*;
182 see Methods). We focused on the *de novo* assembled contigs that had no significant hits
183 using initial searches against the NCBI nucleotide and non-redundant databases.
184 Accordingly, of 293,586 orphan contigs, 57 contained translatable ORFs of more than
185 1000 nt in length, and because we hypothesized that some may correspond to
186 undetected virus sequences, we interrogated them using a protein structure prediction
187 approach with template-based modelling (TBM) in Phyre2 [27]. From the 57 queried
188 contigs, we obtained a 3D model of a 407 amino acid (1227 bp) contig with a high
189 confidence hit (98.3%) to the RdRp catalytic subunit of a bat influenza A virus (family
190 *Orthomyxoviridae*) (Table 1, Figure 1a-b). The confidence level obtained is indicative of
191 high probability of modelling success between putative homologs. In addition, the
192 alignment coverage between our query and the viral template corresponded to 52% (213
193 residues) of the query sequence, while the proportion of identical amino acids (i.e.
194 sequence identity) was 19% (Table 1).

195 To corroborate these findings, the structural results were compared with those
196 obtained from other analyses based on primary sequence similarity searches against
197 public databases (see Methods) (Table 1). This revealed matches to the RdRp subunit
198 (PB1 gene segment) of different members of the order *Articulavirales*, including the
199 Influenza virus (FLUAV), TiLV, and Infectious salmon anaemia virus (ISAV). Comparisons
200 of the assembled contigs against a custom database containing only members of the
201 *Articulavirales* were then performed to improve sequence alignments. Accordingly, the
202 best hit matches were obtained to TiLV (e-values $<10^{-15}$) (Table 1). To identify additional
203 viral segments, the assembled contigs were aligned to the ten segments of TiLV using
204 DIAMOND. A total of 87 contigs were scored through the entire genome, although we did
205 not recover any significant hit for segments 2-10 likely because they are so divergent in
206 sequence (Table S1).

207 *Sequence alignment and phylogenetic relationships*

208 We tentatively name the new virus identified here as Gecko articulavirus (GECV).
209 Multiple sequence alignment of the RdRp between GECV and other members the order
210 *Articulavirales* identified a number of well conserved amino acid motifs (I-IV) ranging in
211 length from 5-11 amino acids in length (Figure 2). Phylogenetic analysis of the aligned
212 RdRp region revealed that GECV falls within the order *Articulavirales* and, along with TiLV

213 (family *Amnoonviridae*), comprises a distinct monophyletic group. The close relationship
214 between GECV and TiLV was supported by high UFBoot/SH-aLRT values (99%/99%)
215 (Figure 1c). Likewise, estimates of the amino acid identity in the RdRp showed a closer
216 (but still distant) sequence similarity (15.35%) with TiLV than other members of the order
217 *Articulavirales* (Table 2).

218 *Host association and in vitro validation*

219 GECV was initially identified in the pooled sequencing library comprising a mix of
220 several Australian reptile species. To identify the exact host species, we screened each
221 individual species sample separately using RT-PCR and Sanger sequencing. As a result,
222 we detected the presence of the novel GECV RdRp sequence in liver tissue of *G. lauta*
223 (paratype QM J96622) (Figure S1), a gecko species native to north-western Queensland
224 and the north-eastern Northern territory in Australia [30].

225 **Discussion**

226 Advances in protein modelling and sequence analysis based on structural
227 comparisons with well-characterized protein templates constitute an attractive approach
228 for the identification of highly divergent RNA viruses [27]. As viral proteins such as the
229 RdRp play a central role on transcription and replication of RNA viruses, it is expected
230 that structures and key motifs for catalytic functionality will be relatively well conserved
231 throughout evolutionary history [31,32]. Based on this premise, it is expected that
232 template-based protein structure modelling could be a powerful tool in the identification
233 of highly divergent viruses [7,27,33]. Accordingly, we used protein structural similarity in
234 combination with sequence and a profile similarity to identify a novel and divergent RNA
235 virus in an Australian gecko (*G. lauta*).

236 We obtained a confident predicted 3D model for the RdRp of GECV based on its
237 structural similarity with the RdRp subunit PB1 of influenza virus (family *Orthomyxoviridae*)
238 (Figure 1a-b; Table 1). Although the structural data suggested that GECV belonged to the
239 family *Orthomyxoviridae* (order *Articulavirales*) [27], additional sequence analysis revealed
240 a closer relationship to members of the family *Amnoonviridae* (Figure 1c). In this context it
241 is important to recall that biases in taxonomic assignment can occur because of the
242 limited number of available proteins with known structures in the PDB. Although this is
243 clearly a limitation, template-based approaches offer a tractable starting point for virus
244 discovery and its taxonomic classification.

245 Although compromised by the large evolutionary distances involved, phylogenetic
246 analysis among members of the order *Articulavirales* revealed that GECV was most

247 closely related to TiLV, in turn suggesting that GECV is a novel and divergent genus within
248 the *Amnoonviridae*. To date, the family *Amnoonviridae* has only been detected in fish [14],
249 such that the discovery of GECV expands the host range of this family. Indeed, given the
250 distance between the TiLV and GECV viruses, we can expect that further uncharacterised
251 diversity exists in the family *Amnoonviridae* especially in fish and reptiles, and that more
252 studies using the form of genomic surveillance performed here will reveal a far greater
253 diversity of negative-sense RNA viruses [6,34].

254 Comparisons of the RdRp subunit PB1 from different articlaviruses revealed the
255 presence of four well conserved motifs in GECV, broadly consistent with observations
256 made for TiLV [14]. As suggested by several studies, motifs I-IV are critically implicated in
257 the catalytic activity of PB1 [35,36]. Despite minor variations, we identified the SDD
258 (serine-aspartic acid-aspartic acid) sequence in motif III that is presumed to be essential
259 for protein functionality in FLUV [35,36]. Hence, the presence of well conserved motifs I-IV
260 across the order *Articulavirales* may constitute effective molecular fingerprints for these
261 viruses. Unfortunately, the marked lack of sequence similarity meant we did not recover
262 any conclusive evidence regarding presence of other genome segments in GECV. Further
263 studies that include sequencing, microscopy, and cell culture techniques, are therefore
264 required to fully characterize the genome of this novel virus.

265 The identification of a novel virus in an Australian gecko (*G. lauta*) highlights the
266 importance of virus surveillance in native species. Although GECV was detected in liver
267 tissue, we currently cannot draw any conclusions regarding its pathogenic potential and
268 impact on the health of *G. lauta*, particularly since a limited number of individuals were
269 collected and all were apparently healthy. Additional research is therefore needed to
270 establish the type of biological interaction between GECV and *G. lauta*. While a previous
271 study reported the isolation of the arbovirus Charleville virus (family *Rhabdoviridae*) in *G.*
272 *australis* (possibly *G. dubia* based on its distribution) collected in Queensland [36,37], this
273 is the first report of a divergent articlavirus in reptiles. Taken together, these findings hint
274 at a hidden diversity of RNA viruses in reptiles that remains to be characterized.

275 **Figure Legends**

276

277 **Figure 1.** Protein structure prediction and phylogenetic relationships of GECV. **(a)** 3D
278 model prediction of the RdRp subunit PB1 of GECV (top left). Protein structure
279 superposition in the aligned region between the predicted model for GECV and the
280 RdRp (PB1 gene) of influenza A virus (FLUAV) (top right). Protein structure
281 superposition of the predicted model for GECV and the entire RdRp subunit of
282 FLUAV (bottom). The protein structure predicted for GECV is displayed in orange and
283 that of FLUAV in green. **(b)** Confidence summary of residues modelled. **(c)** Maximum
284 likelihood tree depicting the phylogenetic relationships between GECV and TiLV
285 within the family *Amnoonviridae*, order *Articulavirales*. Families are indicated with
286 colored filled bubbles. Tip labels are colored according to genus. Genera comprising
287 multiple species are indicated with unfilled bubbles. Support values $\geq 95\%$ UFBoot
288 and 80% SH-aLRT are displayed with yellow-circle shapes at nodes.

289 *Alphainfluenzavirus* (FLUBA); *Betainfluenzavirus* (FLUBV); *Deltainfluenzavirus* (FLUDV);
290 *Gammainfluenzavirus* (FLUCV); *Dhori thogotovirus* (DHOV); *Oz virus* (OZV); *Thogoto*
291 *thogotovirus* (THOV); *Quaranfil quaranjavirus* (QRFV); *Wellfleet Bay virus* (WFBV);
292 *Johnston Atoll quaranjavirus* (JAV); *Salmon isavirus* (ISAV); *Tilapia tilapinevirus* (TiLV);
293 *Gecko articulavirus* (GECV); *Blueberry mosaic associated virus* (BIMaV); *Montano*
294 *orthohantavirus* (MTNV); *Bayou orthohantavirus* (BAYV).

295 **Figure 2.** Conserved motifs in the RdRp subunit PB1 from the order *Articulavirales*.
296 **(a)** Comparison of the GECV RdRp sequence with the full-length PB1 sequence of
297 TiLV and FLUAV. **(b)** Top panel shows the mean pairwise identity over all pairs in the
298 column across the multiple sequence alignment. The bottom panel depicts the
299 individual motifs. The original amino acid residue position and standard logos are
300 displayed in the top of each motif; the size of each character represents the level of
301 sequence conservation. Amino acid residues in the alignment are coloured according
302 to the Clustal colouring scheme.

303 **Supplementary Materials.**

304 **Figure S1.** PCR detection and host association of GECV. (a-b) Agarose gels
305 electrophoresis showing PCR products from two sets of primers that target a region in
306 the PB1 gene segment (RdRp). Samples correspond to (c) liver tissue from seven different
307 reptile species. A 355 bp PCR product was only amplified in *G. lauta*.

308 **Table S1.** Summary of the contig alignment to genomic segments of TiLV using
309 DIAMOND. The relative abundance of each transcript was also calculated (see Methods).

310 **Table S2.** List of virus sequences used in the phylogenetic analysis. All sequences
311 correspond to the PB1 protein.

312 **Table S3.** Set of primers used for PCR and Sanger sequencing reactions.

313

314

315 **Author Contributions.**

316 Conceptualization, E.C.H.; methodology, A.S.O.-B., E.C.H., and J.-S.E.; formal analysis,
317 A.S.O.-B.; investigation, A.S.O.-B., E.C.H., and J.-S.E.; resources, C.M., J.-S.E and
318 E.C.H. ; writing—original draft preparation A.S.O.-B.; writing—review and editing E.C.H.,
319 J.-S.E. and C.M.; visualization, A.S.O.-B.; supervision, E.C.H. All authors have read and
320 agreed to the published version of the manuscript.

321 **Funding:** This research was funded by the Australian Research Council, grant number
322 FL170100022.

323 **Acknowledgments:** None.

324 **Conflicts of Interest:** The authors declare no conflict of interest.

325

326 **References**

- 327 1. Thermes, C. Ten years of next-generation sequencing technology. *Trends Genet.*
328 **2014**, *30*, 418–426.
- 329 2. Shi, M.; Lin, X.-D.; Chen, X.; Tian, J.-H.; Chen, L.-J.; Li, K.; Wang, W.; Eden, J.-S.;
330 Shen, J.-J.; Liu, L.; Holmes, E.C.; Zhang, Y.-Z. The evolutionary history of vertebrate
331 RNA viruses. *Nature* **2018**, *556*, 197–202.
- 332 3. Zhang, Y.-Z.; Chen, Y.-M.; Wang, W.; Qin, X.-C.; Holmes, E.C. Expanding the RNA
333 virosphere by unbiased metagenomics. *Annu. Rev. Virol.* **2019**, *6*, 119–139.
- 334 4. Zhang, Y.-Z.; Shi, M.; Holmes, E.C. Using metagenomics to characterize an
335 expanding virosphere. *Cell* **2018**, *172*, 1168–1172.
- 336 5. Rose, R.; Constantinides, B.; Tapinos, A.; Robertson, D.L.; Prospero, M. Challenges in
337 the analysis of viral metagenomes. *Virus Evol.* **2016**, *2*, vew02,.
- 338 6. Shi, M.; Lin, X.-D.; Vasilakis, N.; Tian, J.-H.; Li, C.-X.; Chen, L.-J.; Eastwood, G.; Diao,
339 X.-N.; Chen, M.-H.; Chen, X.; Qin, X.-C.; Widen, S.G.; Wood, T.G.; Tesh, R.B.; Xu, J.;
340 Holmes, E.C.; Zhang, Y.-Z. Divergent viruses discovered in arthropods and
341 vertebrates revise the evolutionary history of the *Flaviviridae* and related viruses. *J.*
342 *Virol.* **2016**, *90*, 659–669.
- 343 7. Deng, H.; Jia, Y.; Zhang, Y. Protein structure prediction. *Int. J. Mod. Phys. B* **2018**,
344 *32*.
- 345 8. Holmes, E.C. What does virus evolution tell us about virus origins? *J. Virol.* **2011**, *85*,
346 5247–5251.
- 347 9. Bamford, D.H.; Grimes, J.M.; Stuart, D.I. What does structure tell us about virus
348 evolution? *Curr. Opin. Struct. Biol.* **2005**, *15*, 655–663.
- 349 10. Benson, S.D.; Bamford, J.K.H.; Bamford, D.H.; Burnett, R.M. Does common
350 architecture reveal a viral lineage spanning all three domains of life? *Mol. Cell* **2004**,
351 *16*, 673–685.
- 352 11. Rice, G.; Tang, L.; Stedman, K.; Roberto, F.; Spuhler, J.; Gillitzer, E.; Johnson, J.E.;
353 Douglas, T.; Young, M. The structure of a thermophilic archaeal virus shows a
354 double-stranded DNA viral capsid type that spans all domains of life. *Proc. Natl.*
355 *Acad. Sci. U.S.A.* **2004**, *101*, 7716–7720.
- 356 12. Baker, D.; Sali, A. Protein structure prediction and structural genomics. *Science*
357 **2001**, *294*, 93–96.
- 358 13. Shi, M.; Lin, X.D.; Tian, J.H.; Chen, L.J.; Chen, X.; Li, C.X.; Qin, X.C.; Li, J.; Cao, J.P.;
359 Eden, J.S.; Buchmann, J.; Wang, W.; Xu, J.; Holmes, E.C.; Zhang, Y.Z. Redefining the
360 invertebrate RNA virosphere. *Nature* **2016**, *540*, 539–543.

- 361 14. Bacharach, E.; Mishra, N.; Briese, T.; Zody, M.C.; Kembou Tsofack, J.E.; Zamostiano,
362 R.; Berkowitz, A.; Ng, J.; Nitido, A.; Corvelo, A.; Toussaint, N.C.; Abel Nielsen, S.C.;
363 Hornig, M.; Del Pozo, J.; Bloom, T.; Ferguson, H.; Eldar, A.; Lipkin, W.I.
364 Characterization of a novel orthomyxo-like virus causing mass die-offs of Tilapia.
365 *mBio* **2016**, 7, e00431-16.
- 366 15. Jansen, M.D.; Dong, H.T.; Mohan, C.V. Tilapia Lake Virus: a threat to the global
367 Tilapia industry? *Rev. Aquac.* **2019**, 11, 725–739.
- 368 16. Pulido, L.L.H.; Mora, C.M.; Hung, A.L.; Dong, H.T.; Senapin, S. Tilapia Lake Virus
369 (TiLV) from Peru is genetically close to the Israeli isolates. *Aquaculture* **2019**, 510, 61–
370 65.
- 371 17. Ahasan, M.S.; Keleher, W.; Giray, C.; Perry, B.; Surachetpong, W.; Nicholson, P.; Al-
372 Hussinee, L.; Subramaniam, K.; Waltzek, T.B. Genomic characterization of Tilapia
373 Lake Virus isolates recovered from moribund Nile Tilapia (*Oreochromis niloticus*) on a
374 farm in the United States. *Microbiol. Resour. Announc.* **2020**, 9, e01368-19.
- 375 18. Subramaniam, K.; Ferguson, H.W.; Kabuusu, R.; Waltzek, T.B. Genome sequence of
376 Tilapia Lake Virus associated with syncytial hepatitis of Tilapia in an Ecuadorian
377 aquaculture facility. *Microbiol. Resour. Announc.* **2019**, 8, e00084-19.
- 378 19. Al-Hussinee, L.; Subramaniam, K.; Ahasan, M.S.; Keleher, B.; Waltzek, T.B. Complete
379 genome sequence of a Tilapia Lake Virus isolate obtained from Nile tilapia
380 (*Oreochromis Niloticus*). *Genome Announc.* **2018**, 6, e00580-18.
- 381 20. Payne, S. Family *Orthomyxoviridae*. In *Viruses*; Elsevier, 2017; pp 197–208.
- 382 21. Bolger, A.M.; Lohse, M.; Usadel, B. Trimmomatic: a flexible trimmer for Illumina
383 sequence data. *Bioinformatics* **2014**, 30, 2114–2120.
- 384 22. Grabherr, M.G.; Haas, B.J.; Yassour, M.; Levin, J.Z.; Thompson, D.A.; Amit, I.;
385 Adiconis, X.; Fan, L.; Raychowdhury, R.; Zeng, Q.; Chen, Z.; Mauceli, E.; Hacohen,
386 N.; Gnirke, A.; Rhind, N.; di Palma, F.; Birren, B.W.; Nusbaum, C.; Lindblad-Toh, K.;
387 Friedman, N.; Regev, A. full-length transcriptome assembly from RNA-Seq data
388 without a reference genome. *Nat. Biotechnol.* **2011**, 29, 644–652.
- 389 23. Li, B.; Dewey, C.N. RSEM: Accurate transcript quantification from RNA-Seq data with
390 or without a reference genome. *BMC Bioinformatics* **2011**, 12, 323.
- 391 24. Altschul, S.F.; Gish, W.; Miller, W.; Myers, E.W.; Lipman, D.J. Basic Local Alignment
392 Search Tool. *J. Mol. Biol.* **1990**, 215, 403–410.
- 393 25. Buchfink, B.; Xie, C.; Huson, D.H. Fast and sensitive protein alignment using
394 DIAMOND. *Nat. Methods* **2015**, 12, 59–60.
- 395 26. Rice, P.; Longden, L.; Bleasby, A. EMBOSS: The European Molecular Biology open
396 software suite. *Trends Genet.* **2000**, 16, 276-277.

- 397 27. Kelley, L.A.; Mezulis, S.; Yates, C.M.; Wass, M.N.; Sternberg, M.J.E. The Phyre2 web
398 portal for protein modeling, prediction and analysis. *Nat. Protoc.* **2015**, *10*, 845–858.
- 399 28. Katoh, K.; Standley, D.M. MAFFT Multiple Sequence Alignment Software Version 7:
400 improvements in performance and usability. *Mol. Biol. Evol.* **2013**, *30*, 772–780.
- 401 29. Nguyen, L.-T.; Schmidt, H.A.; von Haeseler, A.; Minh, B.Q. IQ-TREE: A fast and
402 effective stochastic algorithm for estimating maximum-likelihood phylogenies. *Mol.*
403 *Biol. Evol.* **2015**, *32*, 268–274.
- 404 30. Oliver, P.M.; Prasetya, A.M.; Tedeschi, L.G.; Fenker, J.; Ellis, R.J.; Doughty, P.;
405 Moritz, C. Cripsis and convergence: integrative taxonomic revision of the *Gehyra*
406 *Australis* group (Squamata: Gekkonidae) from Northern Australia. *PeerJ* **2020**, *2020*,
407 e7971.
- 408 31. Zanotto, P.M. de A.; Gibbs, M.J.; Gould, E.A.; Holmes, E.C. A reevaluation of the
409 higher taxonomy of viruses based on RNA polymerases. *J. Virol.* **1996**, *70*, 6083-
410 6096..
- 411 32. Ng, K.K.S.; Arnold, J.J.; Cameron, C.E. Structure-function relationships among RNA-
412 dependent RNA polymerases. *Curr. Top. Microbiol. Immunol.* **2008**, *320*, 137–156.
- 413 33. Fiser, A. Template-based protein structure modeling. *Methods in molecular biology*
414 *(Clifton, N.J.)*. Humana Press, Totowa, NJ **2010**, pp 73–94.
- 415 34. Li, C.-X.; Shi, M.; Tian, J.-H.; Lin, X.-D.; Kang, Y.-J.; Chen, L.-J.; Qin, X.-C.; Xu, J.;
416 Holmes, E.C.; Zhang, Y.-Z. Unprecedented genomic diversity of RNA viruses in
417 arthropods reveals the ancestry of negative-sense RNA viruses. *eLife* **2015**, *4*,
418 e05378.
- 419 35. Biswas, S.K.; Nayak, D.P. Mutational analysis of the conserved motifs of influenza A
420 virus polymerase basic protein 1. *J. Virol.* **1994**, *68*, 1819–1826.
- 421 36. Chu, C.; Fan, S.; Li, C.; Macken, C.; Kim, J.H.; Hatta, M.; Neumann, G.; Kawaoka, Y.
422 Functional analysis of conserved motifs in influenza virus PB1 protein. *PLoS One*
423 **2012**, *7*, e36113.
- 424

425 **Table 1.** Summary of analyses and parameters used for the detection of GECV.

Analysis/database	Parameter (unit)	Value / Hit (e-value)
Trinity <i>de novo</i> assembly	Length (nt)	1227
	Predicted ORF length (aa)	407
	Coverage (# of reads)	35
	Abundance (TPM ¹)	1.10
Phyre2/PDB	PDB molecule	RdRp catalytic subunit
	PDB title	Bat influenza a polymerase with bound vRNA promoter
	PDB identifier	4WSB
	Resolution	2.65
	Confidence (%)	98.3
	Coverage (%)	52
	Identity (%)	19
DIAMOND/nr	Match	Hypothetical protein (Tilapia lake virus), segment 1
	Similarity (%)	29
	E-value	1.30E-07
DIAMOND/custom db	Match	Hypothetical protein (Tilapia lake virus), segment 1
	Similarity (%)	29
	E-value	2.4E-14
HMMER/references proteomes	Taxonomy	Tilapia lake virus (3.9e-11)
	Domain architecture	Flu_PB1
HMMER/UniProt	Taxonomy	Tilapia lake virus (1.4e-10)
	Domain architecture	Flu_PB1
HMMER/SwissProt	Taxonomy	Infectious salmon anaemia virus RDRP_ISAV8, segment 2 (5.2e-3)
	Domain architecture	Flu_PB1
Pfam	Family	Flu_PB1 (1.8e-2)
	Description	Influenza RNA-dependent RNA polymerase subunit PB1
CDD/CDDv3.17	Domain hit	Flu_PB1 super family (6.43e-05)

426 ¹TPM: transcripts per million.

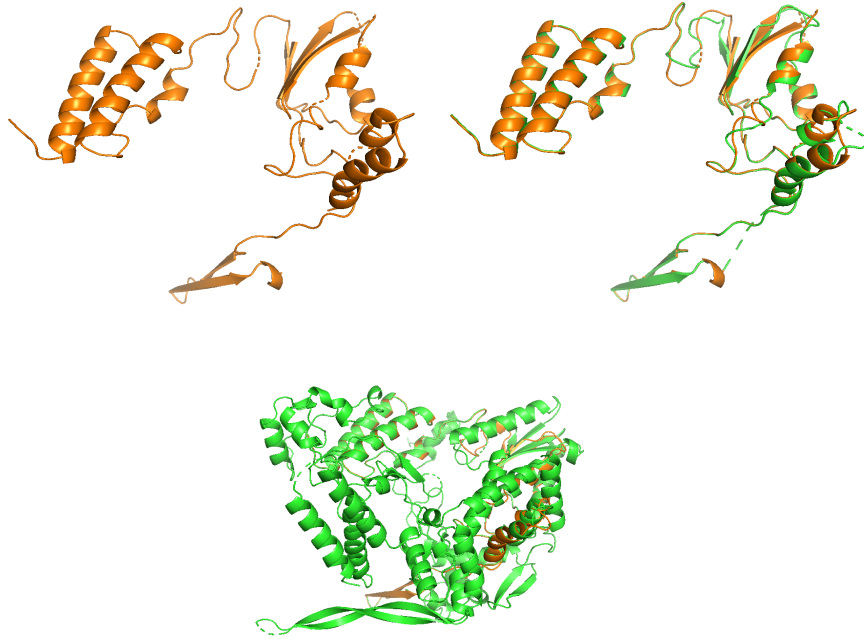
427 **Table 2.** Percentage of identical residues among members of the order *Articulavirales*
 428 and GECV.

Virus classification			Percentage of amino acid identity ¹		
Family	Genus	Species	FLUAV	TiLV	GECV
<i>Orthomyxoviridae</i>	<i>Alphainfluenzavirus</i>	FLUAV	--	13.90	11.75
	<i>Betainfluenzavirus</i>	FLUBV	60.37	13.33	12.01
	<i>Deltainfluenzavirus</i>	FLUDV	39.03	14.62	11.53
	<i>Gammainfluenzavirus</i>	FLUCV	38.63	14.50	12.66
	<i>Isavirus</i>	ISAV	18.40	11.84	11.41
	<i>Quaranjavirus</i>	QRFV	22.94	13.68	11.46
	<i>Thogotovirus</i>	THOV	24.90	14.61	13.08
<i>Amnoonviridae</i>	<i>Tilapinevirus</i>	TiLV	13.90	--	15.35

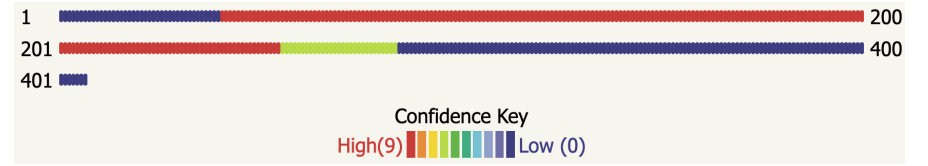
429 ¹ Percentage of identical bases/residues

430

a



b



c

